NATURAL CONVECTION IN A PARTIALLY DIVIDED TRAPEZOIDAL CAVITY USING THE ELEMENT BASED FINITE VOLUME METHOD

André Luiz de Souza Araújo, andre@cefetce.br
Federal Center of Technological Education of Ceara
13 de Maio, 2081
60040-531
Fortaleza, Brazil

José Maurício Alves de Matos Gurgel, gurgel@les.ufpb.br
Mechanical Technology Department
Federal University of Paraíba
P.O. Box 5115
58051-970
João Pessoa, Brazil

Francisco Marcondes, marcondes@ufc.br
Mechanical Engineering Department
Federal University of Ceara
P.O. Box 12.144
60.455-760
Fortaleza, Brazil

Abstract. *Although buoyancy-driven flows in regular-shaped cavities have been widely investigated, little attention has been given to the natural convection in enclosures with irregular geometries, which arises in several practical engineering applications. This work presents a numerical study of natural convection in partially divided trapezoidal cavities representing industrial buildings, using an Element based Finite Volume Method (EbFVM). The effect of Rayleigh number as well as the height and position of a baffle inside the cavity will be investigated. In this procedure, quadrilateral elements are employed to discretize the governing equations which are solved simultaneously. The results are displayed in terms of average Nusselt number, isotherms and streamlines*.

Keywords: *natural convection, trapezoidal cavity, unstructured grid, Element based Finite Volume Method.*

1. INTRODUCTION

Natural-convection heat transfer in regular enclosures (rectangular, cylindrical, annulus) has been widely studied. However, buoyancy-driven flows in cavities of irregular geometry have not received the same attention, although such problems arise in many practical situations, such as solar heating and nuclear waste disposal. The non-linear nature of the governing equations associated with the irregular boundaries of the physical domain makes each solution specific to the corresponding configuration (Moukalled and Darwish, 2003).

This work presents the solution of the natural convection in partially divided trapezoidal cavities, heated from the side. The governing equations are solved by the Element based Finite Volume Method (EbFVM) in conjunction with quadrilateral elements. This numerical scheme, developed by Raw (1985), combines the features of two others classic formulations: the Finite Volume Method (FVM) and the Finite Element Method (FEM). In this approach, the physical domain is broken up into quadrilateral elements and each element is divided into four sub-control volumes. The conservation equations are then integrated over each sub-control volume. Also, the transport equations are solved simultaneously.

The results for several Rayleigh numbers are presented in terms of average Nusselt number, isotherms and streamlines. The effect of a baffle in the heat transfer process is also considered. Finally, these results are compared to those obtained by Moukalled and Darwish (2003) using a traditional control-volume method.

2. MATHEMATICAL MODEL

The governing equations of mass, momentum and energy, representing a two-dimensional, incompressible and laminar flow, using the Einstein notation, are, respectively, given by

$$\frac{\partial}{\partial x_j}\left(\rho u_j\right) = 0 \tag{1}$$

$$\frac{\partial}{\partial t}(\rho u_i) + \frac{\partial}{\partial x_j}(\rho u_j u_i) = -\frac{\partial p}{\partial x_i} + \frac{\partial}{\partial x_j}\left[\mu\left(\frac{\partial u_i}{\partial x_j} + \frac{\partial u_j}{\partial x_i}\right)\right] + s_{ui} \tag{2}$$

$$\frac{\partial}{\partial t}(\rho T) + \frac{\partial}{\partial x_j}(\rho u_j T) = \frac{\partial}{\partial x_j}\left(\frac{k}{c_p}\frac{\partial T}{\partial x_j}\right) + s_T \tag{3}$$

where i and j range from 1 to 2, ρ is the specific mass, μ is the viscosity, u_j are the Cartesian components of velocity vector, p is the thermodynamic pressure, T is the temperature, s_{ui} and s_T are, respectively, the source terms of the momentum and energy equations. For the natural convection problem, using the Boussinesq approximation, the source term of the momentum equation is given by:

$$s_{u2} = s_v = \rho g \beta\left(T - \overline{T}\right) \tag{4}$$

where β is the coefficient of thermal expansion of fluid, $\overline{T}$ is the reference temperature (the value $\overline{T}$ = 0.5 has been adopted) and g is the gravitational acceleration.

3. NUMERICAL METHODOLOGY- THE ELEMENT BASED FINITE VOLUME METHOD (EbFVM)

The fundamentals of the Element based Finite Volume Method (EbFVM) are now presented. Further details can be found in Raw (1984), Raw and Schneider (1986), Souza (2000) and Araújo (2004). As it was discussed earlier, this methodology solves the transport equations simultaneously, combining the features of the Finite Volume Method (FVM) and the Finite Element Method (FEM). The algebraic equations are obtained through the application of the conservation laws to an appropriate control volume. Also, the scheme has the ability to describe complex geometries, employing unstructured grids.

3.1. Discretization of the physical domain

The solution domain is divided into smaller domains, called finite elements, which are irregular quadrilaterals. Nodes are located at every element corner and all the problem unknowns (Cartesian components of velocity vector, pressure and temperature) are stored at these nodes. A local, non-orthogonal coordinate system s-t is defined within each element, which is dealt with in isolation. The s and t coordinates range from -1 to 1, and the nodes are numbered 1 to 4 as shown in Fig. 1.

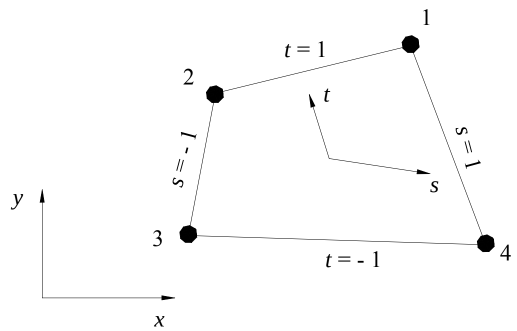

Figure 1. Element definition.

The element is called "isoparametric" since the same functions are used to interpolate physical and geometric information within the element. Using this idea, any variable inside the element can be determined by

$$\Phi(s, t) = \sum_{i=1}^{4} N_i(s, t)\Phi_i \tag{5}$$

where Φ represents a generic variable, Φ_i is its value at the i-node of the element and the $N_i(s, t)$ functions, called shape functions, are given by

$$N_1(s, t) = \frac{1}{4}(1 + s)(1 + t) \tag{6}$$

$$N_2(s,t) = \frac{1}{4}(1-s)(1+t) \tag{7}$$

$$N_3(s,t) = \frac{1}{4}(1-s)(1-t) \tag{8}$$

$$N_4(s,t) = \frac{1}{4}(1+s)(1-t) \tag{9}$$

The derivatives of Φ in terms of the global coordinates x and y are defined as

$$\left.\frac{\partial \Phi}{\partial x}\right|_{(s,t)} = \sum_{i=1}^{4} \left.\frac{\partial N_i}{\partial x}\right|_{(s,t)} \Phi_i \tag{10}$$

$$\left.\frac{\partial \Phi}{\partial y}\right|_{(s,t)} = \sum_{i=1}^{4} \left.\frac{\partial N_i}{\partial y}\right|_{(s,t)} \Phi_i \tag{11}$$

where,

$$\frac{\partial N_i}{\partial x} = \frac{1}{J}\left(\frac{\partial N_i}{\partial s}\frac{\partial y}{\partial t} - \frac{\partial N_i}{\partial t}\frac{\partial y}{\partial s}\right) \tag{12}$$

$$\frac{\partial N_i}{\partial y} = \frac{1}{J}\left(\frac{\partial N_i}{\partial t}\frac{\partial x}{\partial s} - \frac{\partial N_i}{\partial s}\frac{\partial x}{\partial t}\right) \tag{13}$$

and J is the Jacobian of the transformation between the x-y and s-t systems. The expression of J is given by

$$J = \frac{\partial x}{\partial s}\frac{\partial y}{\partial t} - \frac{\partial x}{\partial t}\frac{\partial y}{\partial s} \tag{14}$$

The expressions for the derivatives of the shape functions in terms of s and t are obtained directly from the Eq. (6) to (9).

In order to establish the system of algebraic equations, a control volume is created for each node. Thefore, the $s = 0$ and $t = 0$ lines of the elements surrounding each node are chosen as the volume edges (Fig. 2).

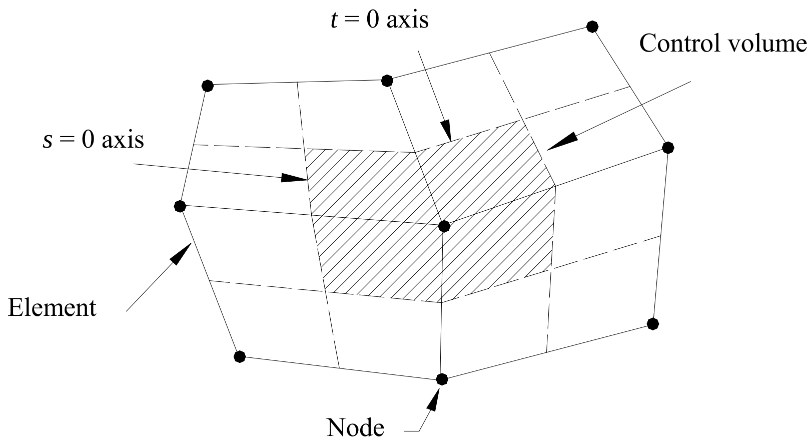

Figure 2. Control volume definition.

Each element contains four control volumes quadrants from four different control volumes, called sub-control-volumes (SCV), which can be seen in Fig. 3a. The discretization of the governing equations requires that several integrations be performed over the control volume surface. These integrals are approximated at the midpoint of the line segments that define the control volume contour (Fig. 3b). The line segments are called sub-surfaces (SS) and their midpoints are referred as integration points (ip's).

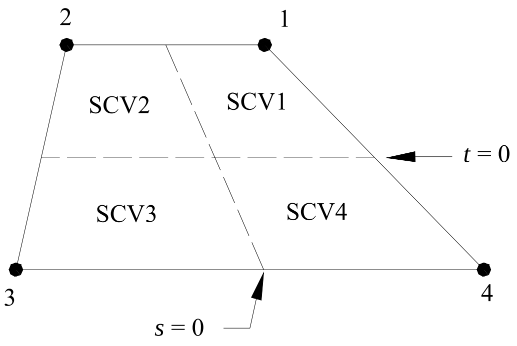

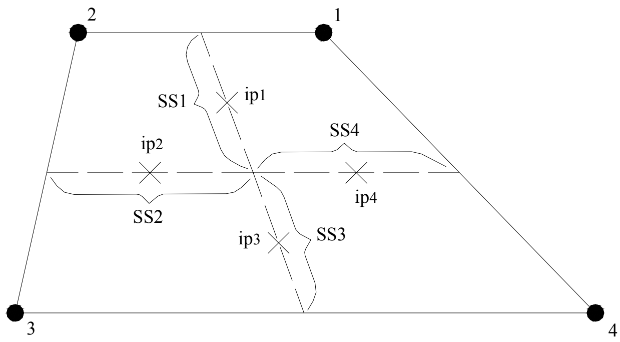

Figure 3. a) Sub-control-volume definition. b) Integration point definition.

3.2. Discretization of the governing equations

A briefly description of the discretization process of the governing equations is now presented. The x-momentum equation is used, and only the SCV1 is considered, which has two sub-surfaces, SS1 and SS4 (Fig. 3a). The notation system employed is that all node variables are upper case and all integration point variables are lower case. The first superscript denotes the equation type (u, for the x-momentum equation, for example), the second one identifies the variable type the coefficient is multiplying. The superscripts c, d, t and s refer to, respectively, the convective, diffusion, transient and source terms, while the first subscript denotes the SCV number and the second one, the node or integration point number the variable is multiplying (depending on the way its symbol is written, upper or lower case).

Integrating Eq. 2 over a control volume and using the Gauss theorem for the advective term the following equation arises:

$$\int_A \frac{\partial}{\partial t}(\rho u_i)dA+\int_S (\rho u_j u_i)dn_j-\int_S \mu\left(\frac{\partial u_i}{\partial x_j}+\frac{\partial u_j}{\partial x_i}\right)dn_j+\int_S p dn_i-\int_A s_{u_i}dA=0 \tag{15}$$

where $d\vec{n}=-dx\vec{i}+dy\vec{j}$ is the outward normal vector to the control sub-surface. The x-momentum equation arises when $i = 1$ and taking the SVC 1 (Fig. 3), for instance, gives

$$\int_{SVC1} \frac{\partial}{\partial t}(\rho u)dA \approx \rho J_1\left(\frac{U_1-U_1^0}{\Delta t}\right)\equiv\sum_{j=1}^{4}A_{1,j}^{uut}U_j-B_1^{ut} \tag{16}$$

$$-\int_{SVC1} s_u\, dA \approx -s_u\big|_{\left(\frac{1}{2},\frac{1}{2}\right)}J_1\equiv -B_1^{us} \tag{17}$$

$$\int_{SS1\&SS4}(\rho u_j u)dn_j \approx \rho u_1^* u_1\Delta y_1-\rho v_1^* u_1\Delta x_1+\rho u_4^* u_4\Delta y_4-\rho v_4^* u_4 \Delta x_4\equiv\sum_{j=1}^{4}a_{1,j}^{uuc}u_j \tag{18}$$

The superscript "*" in Eq. (18) indicates that the corresponding term is evaluated at the previous iteration. The convective and diffusive fluxes are evaluated at the integration points 1 and 4 (Fig. 3b). The diffusive term at ip_1 is given by

$$\begin{aligned}-\int_{SS1}\mu\left(\frac{\partial u_i}{\partial x_j}+\frac{\partial u_j}{\partial x_i}\right)dn_j &\approx -2\mu\frac{\partial u}{\partial x}\bigg|_{ip1}\Delta y_1+\mu\left(\frac{\partial u}{\partial y}+\frac{\partial v}{\partial x}\right)\bigg|_{ip1}\Delta x_1\equiv\\ &-2\mu\left(\sum_{j=1}^{4}\frac{\partial N_j}{\partial x}\bigg|_{ip1}U_j\right)\Delta y_1+\mu\left[\sum_{j=1}^{4}\left(\frac{\partial N_j}{\partial y}\bigg|_{ip1}U_j+\frac{\partial N_j}{\partial x}\bigg|_{ip1}V_j\right)\right]\Delta x_1\end{aligned} \tag{19}$$

Adding to Eq. (19) a similar term for the SS4 and representing the sum in the compact form yields

$$-\int_{SS1\&SS4} \mu\left(\frac{\partial u_i}{\partial x_j}+\frac{\partial u_j}{\partial x_i}\right) dn_j \equiv \sum_{j=1}^{4} A_{1,j}^{uud}\, U_j + \sum_{j=1}^{4} A_{1,j}^{uvd}\, V_j \tag{20}$$

The pressure term is given by

$$\int_{SS1\&SS4} p\, dn \approx p_1 \Delta y_1 + p_4 \Delta y_4 \equiv \sum_{j=1}^{4} a_{1,j}^{upp}\, p_j \tag{21}$$

Finally, putting all together Eqs. (16) through (21), into Eq. (15), an "equation" for the SCV1 is derived

$$\sum_{j=1}^{4}\left(A_{i,j}^{uut}+A_{i,j}^{uud}\right)U_j + \sum_{j=1}^{4} A_{i,j}^{uvd}\, V_j + \sum_{j=1}^{4} a_{i,j}^{uuc}\, u_j + \sum_{j=1}^{4} a_{i,j}^{upp}\, p_j \doteq B_i^{ut} + B_i^{us} \tag{22}$$

The all four sub-control-volume equations taken together can be written in a matrix form as:

$$\left[A^{uut}+A^{uud}\right]\{U\}+\left[A^{uvd}\right]\{V\}+\left[a^{uuc}\right]\{u\}+\left[a^{upp}\right]\{p\}\doteq\left\{B^{ut}\right\}+\left\{B^{us}\right\} \tag{23}$$

where the brackets designate a square matrix and the braces a column vector.

The values of the horizontal velocity component (*u*) and the pressure (*p*) at the integration points can be expressed in terms of their nodal values using interpolation functions, which are algebraic approximations to the differential equation for the mentioned variables. Using matrix notation, *u* and *p* at the integration points can be written as

$$\{u\}=\left[CC^{uu}\right]\{U\}+\left[CC^{up}\right]\{P\}+\left\{RCC^{u}\right\} \tag{24}$$

$$\{p\}=\left[CC^{pp}\right]\{P\} \tag{25}$$

Inserting Eqs. (24) and (25) into Eq. (23) yields:

$$\left[E^{uu}\right]\{U\}+\left[E^{uv}\right]\{V\}+\left[E^{up}\right]\{P\}\doteq\left\{R^{u}\right\} \tag{26}$$

In Eq. (26), each row in the matrix indicates a sub-control-volume, and each column represents a node. Moreover, this equation represents the discretization of a portion of a control volume (that is why the symbol $\doteq$ was employed**)**. The final equation for the control volume is derived adding all of its portions (i. e. when the elements surrounding the control volume in question are assembled).

4. PHYSICAL MODEL OF THE CAVITY

The trapezoidal enclosure under consideration is shown schematically in Fig. 4. The width of the cavity (L) is 4 times the height (H) of the shortest vertical wall. The inclination of the top of the cavity (θ) is fixed at 15º. The baffle thickness (W_b) is equal to L/20 and its location (L_b) is L/3. Two configurations were studied: one with no baffle, and another partially divided (baffle height $H_b = 2H^*/3$, where H^* is the height of the cavity at the location of the baffle).

The temperatures of the shortest and longest vertical walls are set to 1 and 0, respectively. This condition is called buoyancy-assisting mode, once the height of the cavity increases in the direction of the rising fluid. The inclined and horizontal walls are insulated.

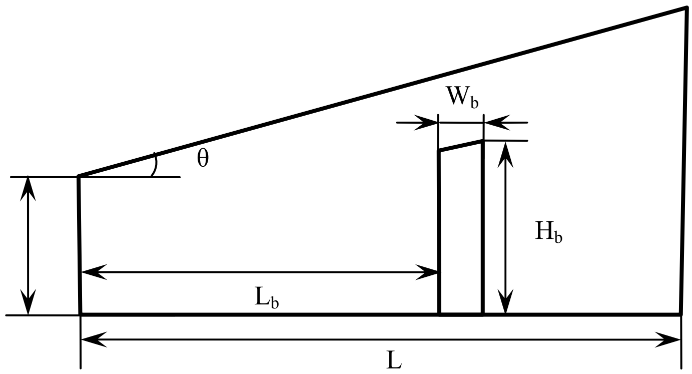

Figure 4. Physical domain.

The confined fluid is air, which properties were evaluated at Pr = 0.7. Rayleigh number equal to 10^3 and 10^4 were considered, based on the height of the shortest vertical wall (H) and on the temperature difference between the vertical walls ($\Delta T = 1$). The ratio between the thermal conductivity of the baffle and the advective fluid is fixed at 2, in order to simulate a poorly conducting divider.

5. SOLUTION PROCEDURE

For all the configurations studied, unstructured grids with nodes clustered closely to the vertical walls were employed, as can be seen in Fig. 5b.

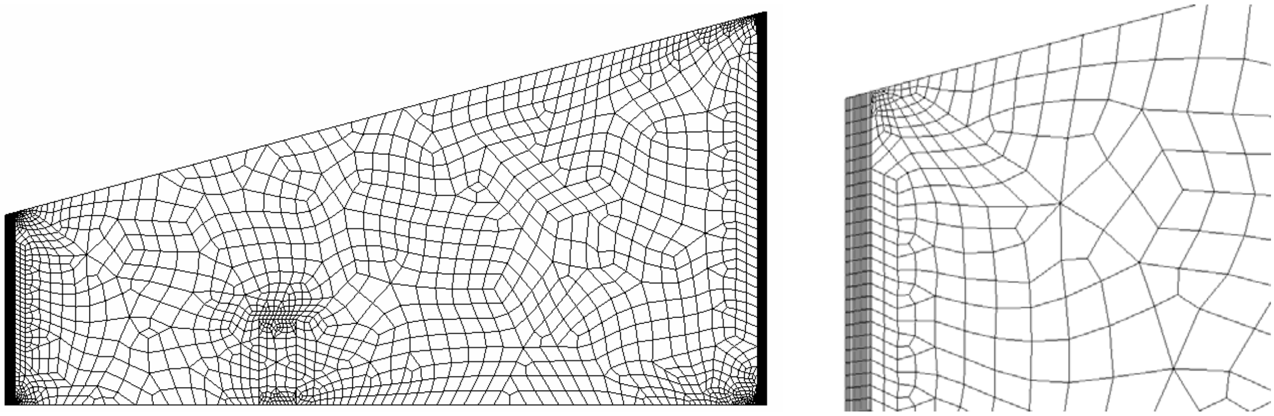

(a) (b)

Figure 5. An unstructured grid with 3980 elements and 4113 nodes employed: a) the whole domain. b) zoom close to the short vertical wall.

The number of nodes was over 4,000 for all configurations analyzed, about the same used by Moukalled and Darwish (2003) using structured meshes. They employed a 68 x 62 structured with concentrated lines close to the boundaries of the cavity.

The baffle region was treated as infinitely viscous fluid (specified numerically as a very large value), which led to zero velocities in this area (Patankar, 1980).

The solution convergence was considered achieved when $\varepsilon_{\vec{u}}$ and $\varepsilon_p < 10^{-4}$, which are calculated by,

$$\varepsilon_{\vec{u}} = \sqrt{\frac{\sum_{i=1}^{N}\left[\left(U_i - U_i^*\right)^2 + \left(V_i - V_i^*\right)^2\right]}{\sum_{i=1}^{N}\left(U_i^2 + V_i^2\right)}} \tag{27}$$

$$\varepsilon_p = \sqrt{\frac{\sum_{i=1}^{N}\left(P_i - P_i^*\right)^2}{\sum_{i=1}^{N} P_i^2}} \tag{28}$$

where * denotes previous iteration and N is the total number of nodes. The velocity and pressure fields were obtained simultaneously, after what the temperature field was solved.

6. RESULTS

Figures 6 and 7 present the isotherms and streamlines in the non-partitioned enclosure. There is a good agreement with the results obtained by Moukalled and Darwish (2003). At low Ra (10^3), isotherms are uniformly distributed over the domain (Fig. 6a and 6b), implying weak advection effects. As Ra increases, isotherms become more distorted, (Fig. 6c and 6d), indicating dominant convection. The flow for the investigated Raleigh, consists of a recirculating eddy as can be seen in Fig. 7.

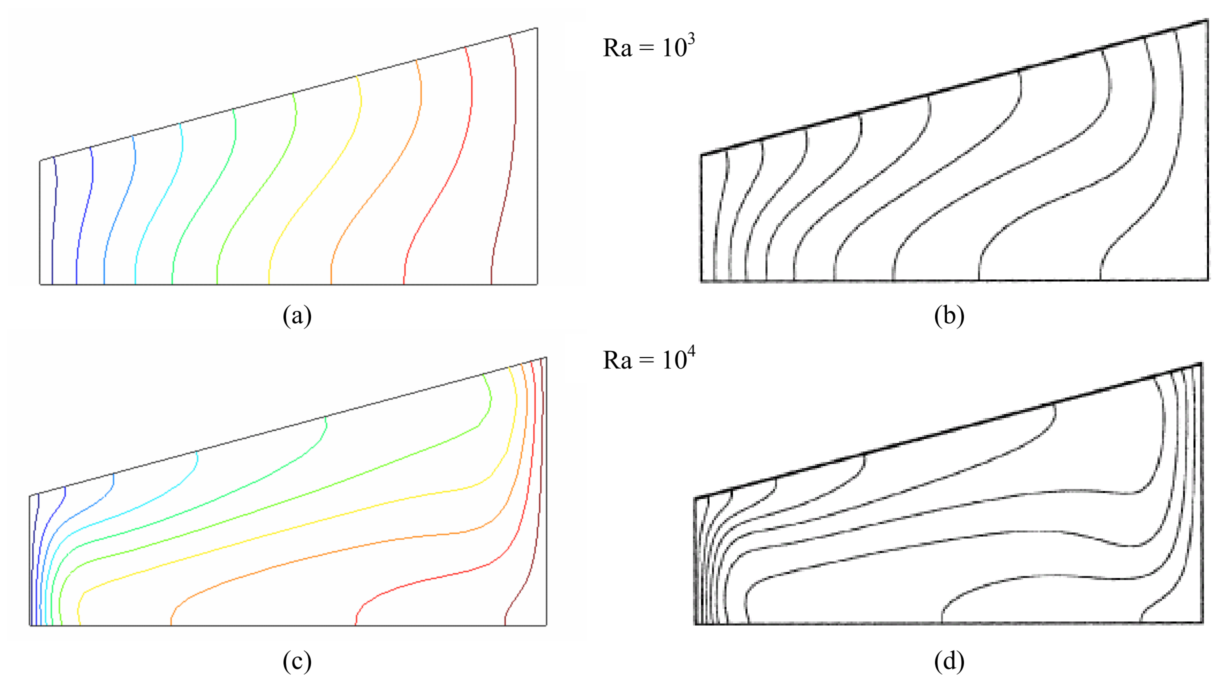

Figure 6. Isotherms in a non-partitioned cavity. a) and c) Present work. b) and d) Moukalled and Darwish (2003).

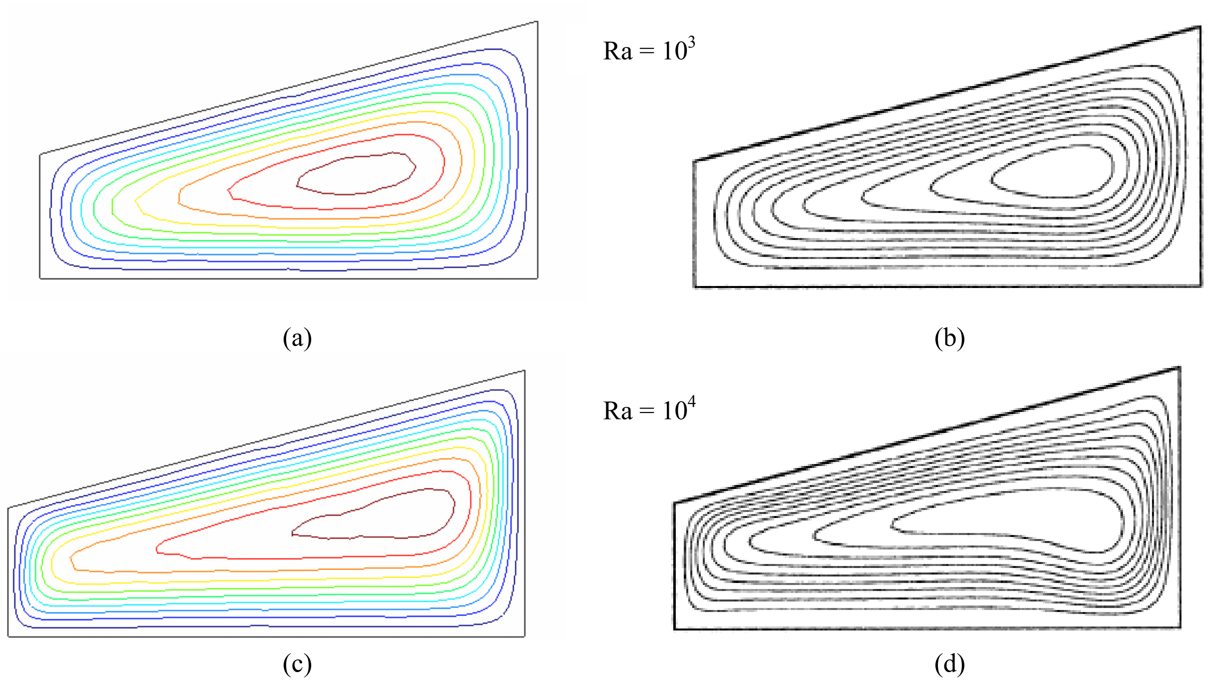

Figure 7. Streamlines in a non-partitione cavity. a) and c) Present work. b) and d) Moukalled and Darwish (2003).

The effect of the baffle on the flow patterns and temperature profiles can be seen in Figs. 8 and 9. Once again, the results present a very good agreement with those obtained by Moukalled and Darwish (2003). At low Ra values, variations in temperature are almost uniform over the domain, indicating a dominant conduction heat transfer mode (Fig. 8a and 8b). As Ra increases, advection becomes more important, thus and isotherms become more distorted (Fig. 8c and 8d). The streamlines, due to the inserting of the baffle consists basically of two separated vortices (Fig. 9).

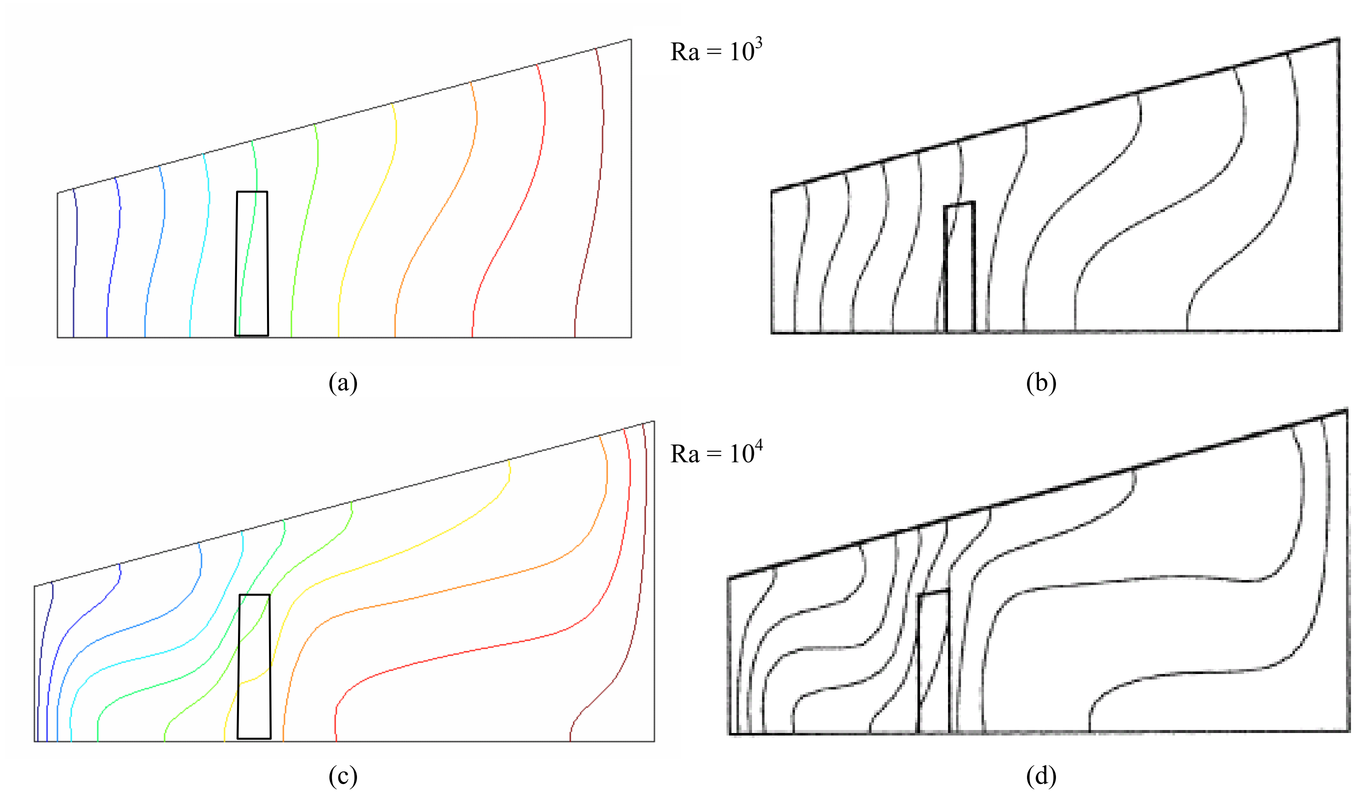

Figure 8. Isotherms in a partitioned cavity. a) and c) Present work. b) and d) Moukalled and Darwish (2003).

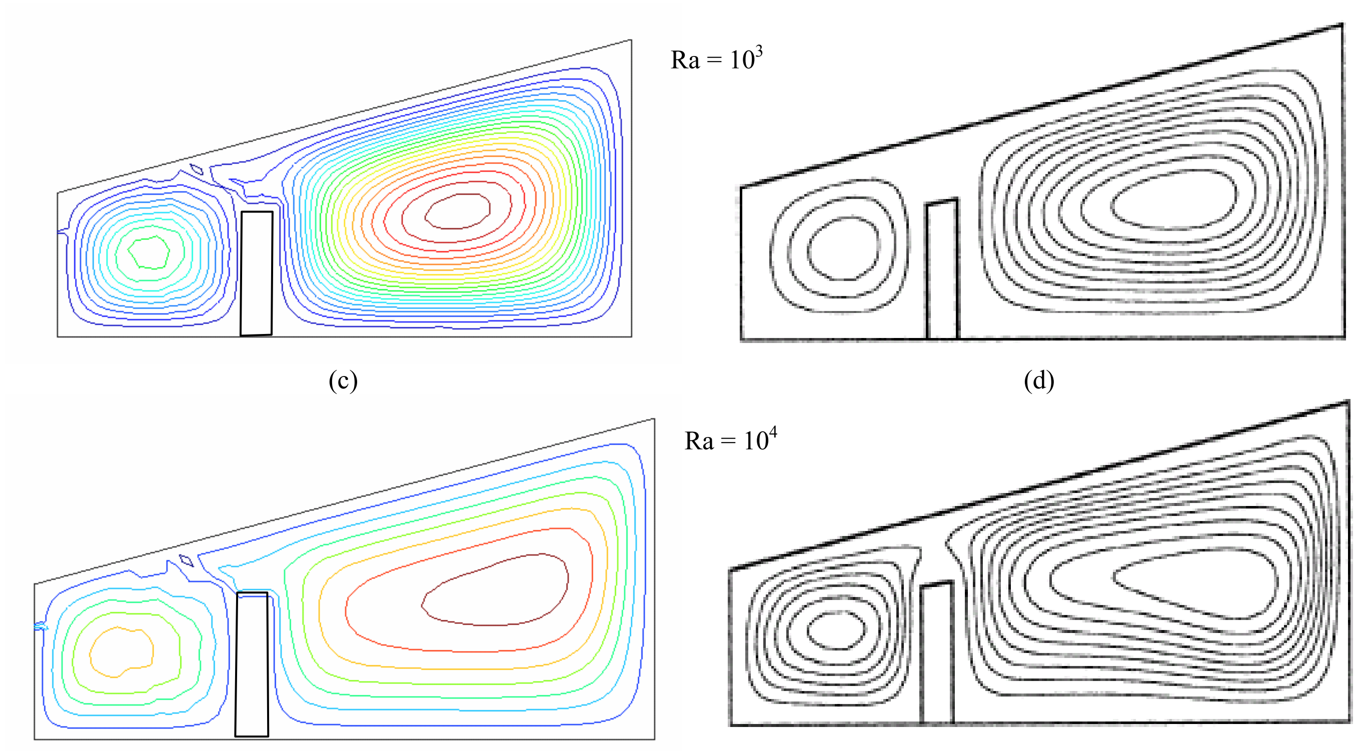

Figure 9. Streamlines in a partitioned cavity. a) and c) Present work. b) and d) Moukalled and Darwish (2003).

Finally, the average Nusselt numbers along the hot and cold wall for all the configurations analyzed are displayed in Tab. 1. According to Moukalled and Darwish, 2003), the expression for the average Nusselt number is given by

$$\overline{Nu} = \frac{1}{l}\int_0^l \frac{hl}{k} dx \tag{29}$$

where l is the height of the shortest or longest vertical wall. From Table 1, it can be verified the average Nusselt numbers present an excellent agreement with those obtained by Moukalled and Darwish (2003).

Table 1. Average Nusselt number values (Pr = 0.7).

Configuration	**Ra**	**Present work**	**Moukalled and Darwish (2003)**
No-baffle	10^3	0.70	0.72
	10^4	2.40	2.48
Baffle	10^3	0.47	0.50
	10^4	1.18	1.13

7. CONCLUSIONS

The problem of natural convection in a partially divided trapezoidal enclosure was solved through the Element based Finite Volume Method (EbFVM) in conjunction with unstructured quadrilateral grids. The momentum mass and energy equations were solved simultaneously for the primitive variables u, v, w, p, and T. The results, in terms of isotherms, streamlines and average Nusselt number, showed an excellent agreement with those obtained by Moukalled and Darwish (2003), using structured grids.

8. ACKNOWLEDGEMENTS

The authors would like to thank CNPq (The National Council for Scientific and Technological Development) for their financial support.

9. REFERENCES

Araújo, A. L. S., “Solução de Escoamentos de Fronteira Livre Usando Malhas Não-Estruturadas e Método dos Volumes Finitos Baseado em Elementos Finitos”, thesis, Federal University of Paraíba, UFPB, Paraíba, Brazil, 2004.

Moukalled F. and Darwish M.,“Natural Convection in a Partitioned Trapezoidal Cavity Heated From The Side”, Numerical Heat Transfer, Part A, 43: 543–563, 2003.

Maliska, C. R., 2004, “Transferência de Calor e Mecânica dos Fluidos Computacional”, LTC, Rio de Janeiro, Brasil.

Patankar, S. V., 1980, “Numerical Heat Transfer and Fluid Flow”, Hemisphere/McGraw-Hill, New York, pp. 96-100.

Raw, M. J., “A New Control-Volume-Based Finite Element Procedure for the Numerical Solution of the Fluid Flow and Scalar Transport Equations”, doctoral thesis, University of Waterloo, 1985.

Raw, M. J. and Schneider, G. E., “A Skewed Positive Influence Coefficient Upwinding Procedure for Control-Volume-Based Finite Element Convection-Diffusion Computation”, *Num. Heat Transfer*, 9, 1-26, 1986.

Souza, J, A., “Implementação de um Método de Volumes Finitos com Sistema de Coordenadas Locais para a Solução Acoplada das Equações de Navier-Stokes”, dissertação de mestrado, Universidade Federal de Santa Catarina, 2000.

10. RESPONSIBILITY NOTICE

The authors are the only responsible for the printed material included in this paper.